

Investigation of the Effect of Different Anchoring Groups in Phenothiazine-Triphenylamine-Based Di-Anchoring Dyes for Dye-Sensitized Solar Cells

Nguyen Thi Hai, Le Quoc Bao, Suresh Thogiti*, Rajesh Cheruku, Kwang-Soon Ahn, and Jae Hong Kim*

Department of Chemical Engineering, Yeungnam University, 214-1, Dae-hakro 280, Gyeongsan, Gyeongsbuk 712-749, Republic of Korea

In dye-sensitized solar cells (DSSCs), as the excited electrons from dye molecules are injected into the conduction band of semiconductor films through the acceptor/anchoring moieties, the acceptor/anchoring groups have significant influences on the photovoltaic properties of the dye sensitizers. This study examined the impacts of different acceptor/anchoring groups (cyanoacetic acid and rhodanine-3-acetic) in phenothiazine-triphenylamine dye sensitizers on the optical, electrochemical photovoltaic performance of DSSCs. The overall conversion efficiency was improved significantly by replacing rhodanine-3-acetic acid (TPAPR) with cyanoacetic acid (TPAPC), which can be attributed to the higher J_{SC} and V_{OC} of the TPAPC device. The lower efficiency of the device based on TPAPR is due mainly to the broken conjugation between the 4-oxo-2-thioxothiazolidine ring and the acetic acid, which affects electron injection from the excited state to the conduction band of TiO_2 . The results are in good agreement with the photovoltaic properties of DSSCs.

Keywords: Dye Sensitized Solar Cells, Electron Acceptor/Anchoring, Electrochemical Properties, Photovoltaic Performance.

1. INTRODUCTION

Dye sensitized solar cells (DSSCs) are promising alternatives to conventional $p-n$ junction solar cells due to low cost and flexible fabrication. The standard structure of a DSSC consists of an electrochemical cell composed of a sensitizer-adsorbed wide band gap semiconductor electrode, an electrolyte containing a red-ox mediator as hole-transporting material, and a Pt-coated counter electrode. The mechanism of a DSSC is based on the injection of electrons from a photosensitizer to the conduction band of a semiconductor. The oxidized photosensitizers are reduced by electron injection from the electrolyte. Therefore, the photosensitizer plays an important role in capturing photons and generating electron/hole pairs, as well as transferring them to the interface of a semiconductor and electrolyte, respectively.¹⁻⁹ The power conversion efficiency is up to 10% using metal-complex sensitizers.¹⁰⁻¹³ Recently, metal-free organic sensitizers have attracted considerable attention because of their great advantages compared to metal sensitizers, such as environment friendly,

high molar extinction coefficients, tunable molecular energy levels, and cost-effectiveness.⁴ Some sensitizers, such as coumarin-indoline-, and triphenylamine-based sensitizers have achieved up to 10% power conversion efficiencies using an iodine-based liquid electrolyte.²³ The donor-(π -bridged)-acceptor (D- π -A) structure is considered to be one of the most promising types of organic sensitizers.^{9,10} When a D- π -A dye molecule is excited, intramolecular charge transfer occurs by the flow of electrons from the donor to the acceptor through a π -bridge, and acceptor carrying functional groups, such as COOH, may strongly bind to the TiO_2 surface. The acceptor also plays an important role that not only transfers excited electrons to the conduction band of the semiconductor, but also adsorbs the sensitizer on the semiconductor. Therefore, the acceptor moiety of the D- π -A molecules should be investigated to achieve better electron transfer and improve the efficiency.¹⁴⁻¹⁹

In this study, two new di-anchoring organic dyes were designed and synthesized and the effects of different acceptor groups (cyanoacetic acid and rhodanine-3-acetic) on the photophysical, electrochemical and photovoltaic

*Authors to whom correspondence should be addressed.

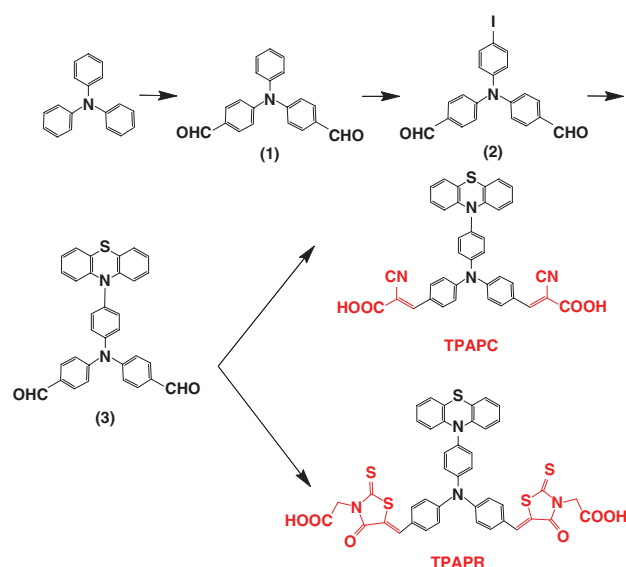


Figure 1. Synthesis procedure for TPAPC and TPAPR.

performance of DSSCs were investigated. Phenothiazine and triphenylamine units were chosen as the donor candidates, as shown in Figure 1.

2. EXPERIMENTAL DETAILS

2.1. Materials and Instrumentation

All starting materials and solvents were purchased from Aldrich-Sigma and used without further purification. The ^1H -nuclear magnetic resonance (NMR) spectra were recorded on a Bruker Advance NMR 300 MHz spectrometer. The UV-Vis spectra were recorded by Cary 5000 UV-Vis-NIR Spectrophotometer. The cyclic voltammograms were estimated with each dye (0.3 mM) and 0.1 mM tetrabutyl ammoniumtetrafluoroborate in a DMF solution, scan rate of 50 mV/s, and three electrodes, Pt, Ag/AgCl, and Pt wire as the working, reference, and counter electrode, respectively.

2.2. Synthesis Procedure

Figure 1 presents the synthetic scheme for the three new sensitizers.

2.3. 4,4'-(phenylazanediyl)Dibenzaldehyde (1)

Triphenylamine (2.45 g, 10 mmol) was dissolved in 1,2-dichloroethane, and DMF (1.8 g, 25 mmol) was then added. The solution was cooled to 0 °C and POCl_3 (3.8 g, 35 mmol) was added drop wise. After color changed to red, the solution was heated under reflux in a nitrogen atmosphere for 6 h. The mixture was diluted with CH_2Cl_2 , rinsed with water and dried with MgSO_4 before being filtered through a silica gel column with a mixture of 70% hexane: 30% CH_2Cl_2 as the eluent to give 4,4'-(phenylazanediyl)dibenzaldehyde as a light yellow solid

(1.59 g, 53%). ^1H MNR (300 MHz, $\text{DMSO}-d_6$) δ 9.89 (s, 2H), 7.86 (d, $J = 8.7$ Hz, 4H), 7.47 (d, $J = 8.1$ Hz, 2H), 7.33 (t, $J = 7.5$ Hz, 1H), 7.23 (d, $J = 7.2$ Hz, 2H), 7.18 (d, $J = 8.7$ Hz, 4H).

2.4. 4,4'-(4-iodophenylazanediyl)Dibenzaldehyde (2)

4,4'-(Phenylazanediyl)dibenzaldehyde (1) (3.01 g, 10 mmol), KI (0.83 g, 5 mmol), and KIO_3 (1.07 g, 5 mmol) dissolved in acetic acid with a small amount of water was placed into a 3 neck 250 ml round bottom flask. The mixture was then heated under reflux for 4 h. The reaction mixture was cooled to room temperature, and water was then added to receive the precipitate. The mixture was then filtered and the precipitate was washed with water to obtain 4,4'-(4-iodophenylazanediyl)dibenzaldehyde (4.06 g, 95%) as a light yellow solid. ^1H MNR (300 MHz, $\text{DMSO}-d_6$) δ 9.872 (s, 2H), 7.83 (d, $J = 8.4$ Hz, 4H), 7.76 (d, $J = 8.4$ Hz, 2H), 7.17 (d, $J = 8.4$ Hz, 4H), 6.98 (d, $J = 8.4$ Hz, 2H).

2.5. 4,4'-(4-(10H-phenothiazin-10-yl)phenylazanediyl)Dibenzaldehyde (3)

Compound (2) (4.27 g, 10 mmol), phenothiazine (5.98 g, 30 mmol), bronze copper (0.38 g, 6 mmol), 18-crown-6 (1 g, 3 mmol) and K_2CO_3 (3.3 g, 25 mmol) were heated under reflux in 1,2-dichlorobenzene for 12 h. Subsequently, the solution was cooled to room temperature, washed with water, and dried with MgSO_4 . The product was isolated on a silica gel column with a mixture of 60% hexane:35% CH_2Cl_2 :5% ethyl acetate as the eluent to give 4,4'-(4-(10H-phenothiazin-10-yl)phenylazanediyl)dibenzaldehyde (3) as a yellow solid (3.14 g, 63%). ^1H MNR (300 MHz, $\text{DMSO}-d_6$) δ 9.902 (s, 2H), 7.88 (d, $J = 8.7$ Hz, 4H), 7.39 (d, $J = 2.4$ Hz, 4H), 7.29 (d, $J = 9.6$ Hz, 4H), 7.11 (d, $J = 7.5$ Hz, 2H), 7.02 (t, $J = 8.5$ Hz, 2H), 6.9 (t, $J = 7.5$ Hz, 2H), 6.42 (d, $J = 8.1$ Hz, 2H).

2.6. 3,3'-(4,4'-(4-(10H-phenothiazin-10-yl)phenylazanediyl)Bis(4,1-phenylene)) Bis(2-cyanoacrylic acid) (TPAPC)

An acetic acid solution of compound 3 (2.45 g, 5 mmol), 2-cyanoacetic acid (1.04 g, 12.5 mmol), and ammonium acetate (0.95 g, 12.5 mmol) was heated under reflux for 10 h. After cooling the mixture to room temperature, the solution was poured into the ice water to allow precipitation. The mixture was filtered and washed with water and then purified on a silica gel column using 95% CHCl_3 :4% methanol:1% acetic acid as the eluent to obtain TPAPC as a yellow solid (2.69 g, 85%). ^1H MNR (300 MHz, $\text{DMSO}-d_6$) δ 7.91 (s, 2H), 7.87 (d, $J = 8.7$ Hz, 4H), 7.35 (d, $J = 2.4$ Hz, 4H), 7.21 (d, $J = 8.7$ Hz, 4H), 7.1 (d, $J = 7.5$ Hz, 2H), 6.99 (t, $J = 7.5$ Hz, 2H), 6.9 (t, $J = 7.5$ Hz, 2H), 6.4 (d, $J = 8.1$ Hz, 2H).

2.7. 2,2'-(5Z,5'Z)-5,5'-(4,4'-(4-(10H-phenothiazin-10-yl)phenylazanediy)Bis(4,1-phenylene))Bis(methan-1-yl-1-ylidene)Bis(4-oxo-2-thioxothiazolidin-3-yl-5-ylidene) Diacetic Acid (TPAPR)

An acetic acid solution of compound 3 (2.45 g, 5 mmol), rhodanine-3-acetic acid (2.35 g, 12.5 mmol), and ammonium acetate (0.95 g, 12.5 mmol) was heated under reflux for 10 h. After cooling the mixture to room temperature, the solution was poured into the ice water to form the precipitate. The mixture was filtered and washed with water, and then purified on a silica gel column using a mixture of 95% CHCl_3 :4% methanol:1% acetic acid as the eluent to obtain TPAPR as an orange solid (3.46 g, 82%). ^1H MNR (300 MHz, $\text{DMSO}-d_6$) δ 7.84 (s, 2H), 7.68 (d, $J = 8.7$ Hz, 4H), 7.41 (d, $J = 2.4$ Hz, 4H), 7.30 (d, $J = 8.7$ Hz, 4H), 7.11 (d, $J = 7.5$ Hz, 2H), 7.03 (t, $J = 7.5$ Hz, 2H), 6.91 (t, $J = 7.5$ Hz, 2H), 6.41 (d, $J = 8.1$ Hz, 2H).

2.8. Solar Cell Fabrication

Fluorine-doped tin oxide (FTO) transparent conducting glass substrates (Pilkington, $15 \Omega/\text{cm}^2$) were cleaned with methanol, D.I water, and acetone. Transparent TiO_2 paste (20–30 nm in diameter, Dyesol Ltd.) was coated on the cleaned FTO glasses (Pilkington, $15 \Omega/\text{cm}^2$) using the doctor blade technique, followed by sintering at 450°C for 30 min. A TiO_2 particle scattering layer (200 nm in diameter, Dyesol Ltd.) was deposited on the transparent nano-porous TiO_2 films, followed by sintering at 450°C for 30 min. Two layers of TiO_2 films were treated with a 40 mM TiCl_4 aqueous solution at 70°C for 30 min and then sintered at 450°C for 30 min. After cooling to 100°C , the TiO_2 films were immersed in 0.3 mM dye solutions at 25°C for 24 h in the dark and the residual dye was rinsed off with acetonitrile to give the working electrode. A platinum paste were deposited on the FTO glasses using the doctor blade technique, followed by sintering at 450°C for 30 min to give the counter electrodes. The working electrode and Pt counter electrodes were assembled into a sealed sandwich cell with a $60 \mu\text{m}$ thick Surlyn film (Dupont), and the cell was filled with an electrolyte solution through pre-drilled holes on the Pt counter electrode. The electrolyte solution consists of 1-butyl-3-methylimidazolium iodide (0.7 M), lithium iodide (LiI, 0.2 M), iodine (I_2 , 0.05 M), and *t*-butylpyridine (TBP, 0.5 M) in acetonitrile/valeronitrile (85:15, v/v).

2.9. Photovoltaic Characterization

The photocurrent density–voltage (J – V) characteristics of the prepared DSSCs were measured under AM 1.5 irradiation with an incident power of $100 \text{ mW}/\text{cm}^2$ (PEC-L11, Peccell Technologies, Inc.). The incident monochromatic photon-to-current efficiencies (IPCEs) were recorded as a function of the light wavelength using an IPCE measurement instrument (PEC-S20, Peccell Technologies, Inc.). Electrochemical impedance

spectroscopy (EIS) was performed using a computer-controlled potentiostat (IVIUMSTAT, IVIUM) at the open circuit voltage with a 10 mV amplitude and an AC frequency range between 100 kHz and 0.1 Hz (PEC-L11, Peccell Technologies, Inc.). The electron diffusion coefficient and electron lifetime of the DSSCs were measured by the stepped light-induced transient measurements of the photocurrent and voltage (SLIM-PCV) using a diode laser (Helium-Neon laser power supply, Thor Lab, $\lambda = 632.8 \text{ nm}$). The current transient was monitored using a digital phosphor oscilloscope (Tektronic DPO 4102B-L) through a current amplifier.

3. RESULTS AND DISCUSSION

3.1. Optical and Electrochemical Properties

Figures 2(a and b) shows the UV-Vis absorption spectra of TPAPC and TPAPR in a DMF solution and on TiO_2 films, respectively. TPAPC in a DMF solution exhibits an absorption band in the range, 300–500 nm, with a molar extinction coefficient (ϵ) of $29,800 \text{ M}^{-1} \text{ cm}^{-1}$ at $\lambda_{\text{max}} = 405 \text{ nm}$ (Table I). TPAPR exhibits two major prominent bands at 300–390 nm and 390–550 nm with molar maximum extinction coefficients of 50, $400 \text{ M}^{-1} \text{ cm}^{-1}$ at $\lambda_{\text{max}} = 405 \text{ nm}$. The absorption peak at approximately 300–390 nm of the TPAPR solution can be assigned to a π – π^* transition and the absorption peak around 390–550 nm is assigned to intramolecular charge transfer (ICT)

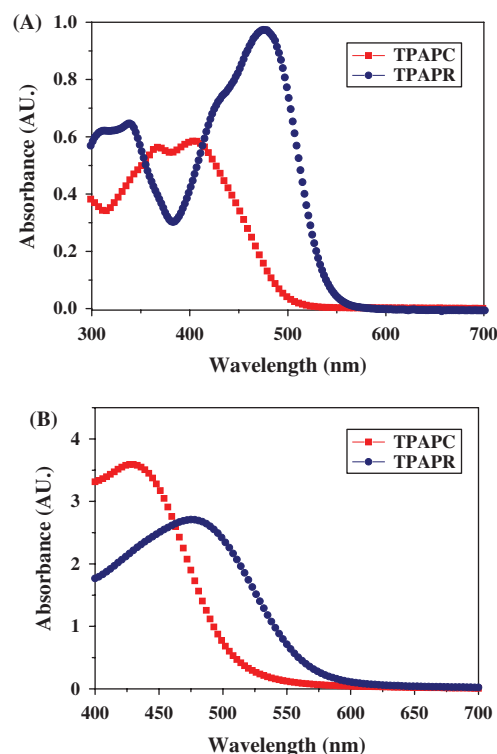


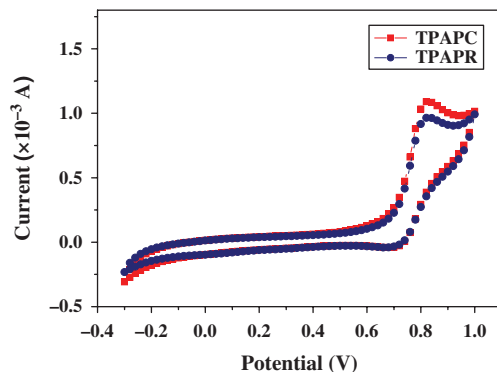
Figure 2. Absorption spectra of TPAPC and TPAPR in a DMF solution (A) and on TiO_2 film (B).

Table I. Optical and electrochemical properties of the TPAPC and TPAPR sensitizers.

Dye	ϵ_{\max} ($M^{-1}cm^{-1}$)	λ_{\max} (nm) solution (TiO_2)	E_{0-0} (eV)	HOMO (eV)	LUMO (eV)
TPAPC	29800	405 (428)	2.51	-5.16	-2.64
TPAPR	50400	476 (478)	2.32	-5.15	-3.82

between the phenothiazine-triphenylamine donor group and the rhodanine-3-acetic acid acceptor group.¹⁰ The absorption band of TPAPR with rhodanine-3-acetic acid as the acceptor in solution shows a red shift compared to that of TPAPC with cyanoacetic acid as the acceptor, which is attributed to the extended π -conjugation system through the 4-oxo-2-thioxothiazolidine ring, leading to a higher electron withdrawal strength of rhodanine-3-acetic acid compared to cyanoacetic acid. In particular, the high molar extinction coefficient of both dyes indicate the good properties for light-harvesting in DSSCs. Based on the absorption spectra of the TPAPC and TPAPR solution, the zeroth-zeroth transition energies (E_{0-0}) (band gap) were estimated to be 2.51 eV and 2.32 eV, respectively.^{20,21} Compared to the absorption spectrum of dyes in solution, the adsorbed-TPAPC on the TiO_2 film exhibited large red shifts ($\Delta\lambda_{\max} \approx 23$ nm), while TPAPR shows a small red shift ($\Delta\lambda_{\max} \approx 2$ nm), which indicates that TPAPC tends to J-aggregate on the electrode surface more than TPAPR. Because of the large size, introducing the rhodanine-3-acetic acid unit as an acceptor in place of cyanoacetic acid leads to a better anti-aggregation effect.

To investigate the molecular orbital energy levels of TPAPC and TPAPR, cyclic voltammetry (CV) was conducted in a dimethylformamide (DMF) solution using 0.1 M tetrabutyl ammonium tetrafluoroborate as the supporting electrolyte (Fig. 3). The highest occupied molecular orbital (HOMO) is estimated from its first oxidation potential (E_{ox}) and the lowest unoccupied molecular orbital (LUMO) is calculated from the expression of

**Figure 3.** Cyclic voltammograms of TPAPC and TPAPR dissolved in DMF.

$LUMO = HOMO - E_{0-0}$. As shown in Table I, the HOMO level of TPAPC and TPAPR are -5.16 eV and -5.15 eV, respectively, which are more positive than the redox potential of I^-/I_3^- (-4.80 eV),¹⁴ making sufficient driving force for the dye regeneration reaction. The LUMO level of TPAPC and TPAPR are -2.64 eV and -3.82 eV, respectively which are more negative than the conduction band of TiO_2 (-4.2 eV), ensuring that the two dyes can inject electrons efficiently from the excited dye molecules to the conduction band of TiO_2 . The LUMO level of TPAPC is more negative than that of TPAPR, indicating the easier electron transfer from the LUMO level of TPAPC to the conduction band of TiO_2 than TPAPR.³

3.2. Photovoltaic Properties

The photovoltaic performance was investigated by the current density-voltage ($J-V$) characteristics of the DSSCs employing TPAPC and TPAPR as the sensitizer under standard global 1.5 AM solar light, 100 mW/cm^2 (Fig. 4(a)); Table II lists the extracted parameters. The overall conversion efficiency (η) of a DSSC is determined by the short circuit current density (J_{sc}), open circuit voltage (V_{oc}), fill factor (FF) of the cell, and intensity of incident light (P_{in}).¹ The FF for DSSC is defined as the ratio of the actual maximum

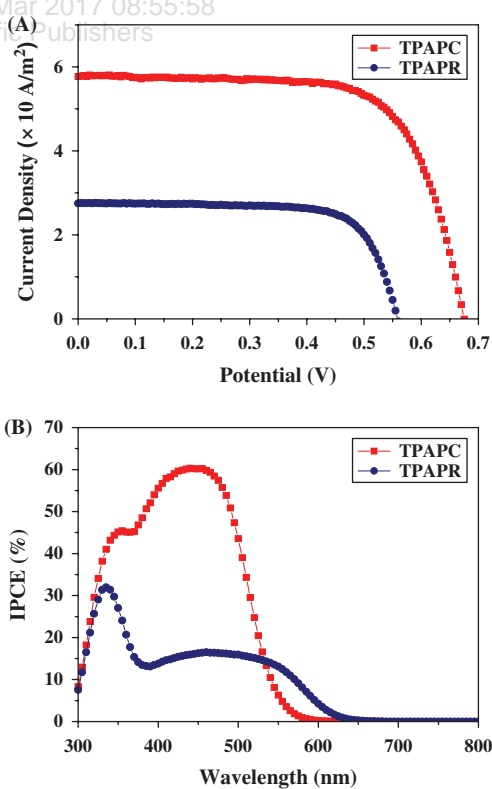
**Figure 4.** $J-V$ characteristics (A) and IPCE (B) spectra of the DSSCs containing TPAPC and TPAPR as a sensitizer under simulated standard solar light illumination (AM 1.5, 100 mW/cm^2).

Table II. Photovoltaic parameters of the TPAPC and TPAPR sensitized DSSCs.

Dye	J_{SC} ($\times 10$ A/m ²)	V_{OC} (V)	FF (%)	η (%)
TPAPC	5.76	0.675	68.53	2.66
TPAPR	2.73	0.558	73.46	1.12

obtainable power ($J_{MP} \times V_{MP}$) to the product of the V_{OC} and J_{SC} .

$$\eta = [J_{SC} \text{ (mA cm}^{-2}\text{)} \times V_{OC} \text{ (V)} \times FF \text{ (\%)}] / P_{in} \text{ (mW cm}^{-2}\text{)} \quad (1a)$$

$$FF = J_{MP} \times V_{MP} / J_{SC} \times V_{OC} \quad (1b)$$

When the TPAPR was used as sensitizer, the solar cell produced a J_{SC} of 2.73 mA/cm², V_{OC} of 0.558 V, and FF of 73.46%, corresponding to a η of 1.12%. Under the same conditions, the TPAPC sensitized solar cell showed higher efficiency (η of 2.66%) which is attributed to the higher J_{SC} (5.76 mA/cm²) and V_{OC} (0.675 V). Figure 4(b) shows incident photon-to-electron conversion efficiencies (IPCE) as a function of the wavelength of the DSSCs using TPAPC and TPAPR as sensitizers in the visible region, 300–800 nm. The IPCE at each incident wavelength was calculated from Eq. (2), where J_{SC} is the short circuit current density under monochromatic irradiation, λ is the wavelength, and Φ is the power of the incident radiation per unit area.²²

$$IPCE = [1240 \text{ (eV nm)} \times J_{SC} \text{ (mA/cm}^{-2}\text{)}] / \lambda \text{ (nm)} \times \Phi \text{ (mW cm}^{-2}\text{)} \quad (2)$$

The TPAPC was active in the wavelength region, 300–550 nm, with the maximum IPCE value of 60% at 440 nm while the TPAPR responses were observed in the range, 300–600 nm, with the maximum IPCE of 16% at 460 nm. As mentioned in the optical properties section, the J -type aggregation effect of sensitizers on the TiO₂ surface results in red-shifts in the spectral range of IPCE compared to the absorption band in solution in both cases of TPAPC and TPAPR. The higher IPCE of TPAPC than TPAPR sensitized solar cell shows correspondence with the higher produced J_{SC} of TPAPC compared to TPAPR. The IPCE is also given by Eq. (3), where LHE is the light harvesting efficiency of the photo electrode (LHE = $1 - 10^{-\alpha d}$, where α is given by the product of the optical absorption cross section and concentration in the meso-porous film of the dye, and d is the film thickness), φ_{inj} is the quantum yield of electron injection, and φ_{coll} is the electron collection efficiency.²²

$$IPCE = LHE \times \varphi_{inj} \times \varphi_{coll} \quad (3)$$

Equation (3) shows that J_{SC} depends not only on the LHE, but also on electron injection and electron transport within the working electrode.

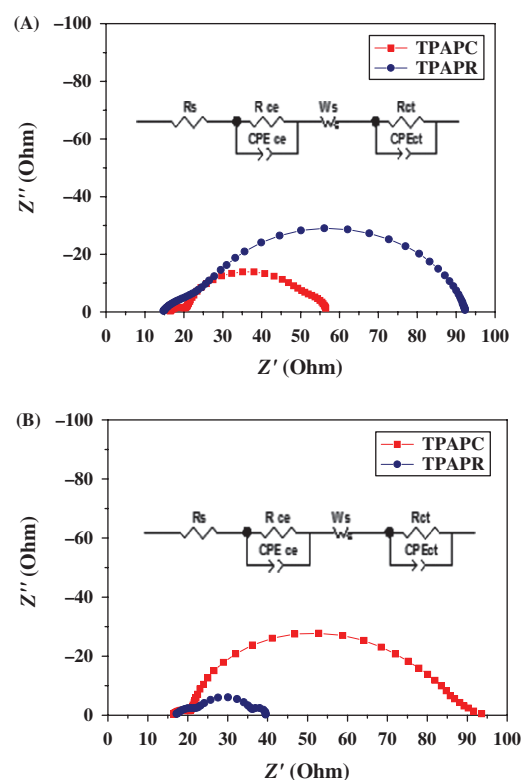


Figure 5. Electrochemical impedance spectroscopy (EIS) of the DSSCs under light illumination (AM 1.5, 100 mW/cm²) (A) and in the dark condition under bias voltage -0.7 V (B). The insets show the equivalent electrochemical circuit of the electrochemical system.

Electrochemical impedance spectroscopy (EIS) and stepped-light induced transient measurements (SLIMs) were conducted to better understand electron injection and electron transport within the working electrode DSSCs using two dyes, TPAPC and TPAPR. Figure 5(a) presents the charge transfer impedance and equivalent electrochemical circuit of the electrochemical system, which was measured under 1.5 AM solar light conditions with a frequency range of 0.1 Hz to 100 kHz. The large semicircle was assigned to the charge transfer impedance (R_{ct}) at the interface of the TiO₂ sensitizer and electrolyte. The R_{ct} (Table III) of the TPAPC sensitized solar cell is 28.7 Ω , which is much lower than that of TPAPR (59.3 Ω), indicating that stronger electronic coupling between the TPAPC dye and TiO₂ than TPAPR leads to higher electron injection efficiency (φ_{inj}) of TPAPC compared to TPAPR. The stepped-light induced transient measurements (SLIMs) were carried out at different light intensities using an on/off laser beam. Under each light

Table III. Electrochemical impedance and SLIM-PCV parameters of the TPAPC and TPAPR sensitized DSSCs.

Dye	R_{ct} (Ω)	R_{rec} (Ω)	L_n ($\times 10^{-6}$ m)
TPAPC	28.7	64.3	12.24
TPAPR	59.3	14.0	10.37

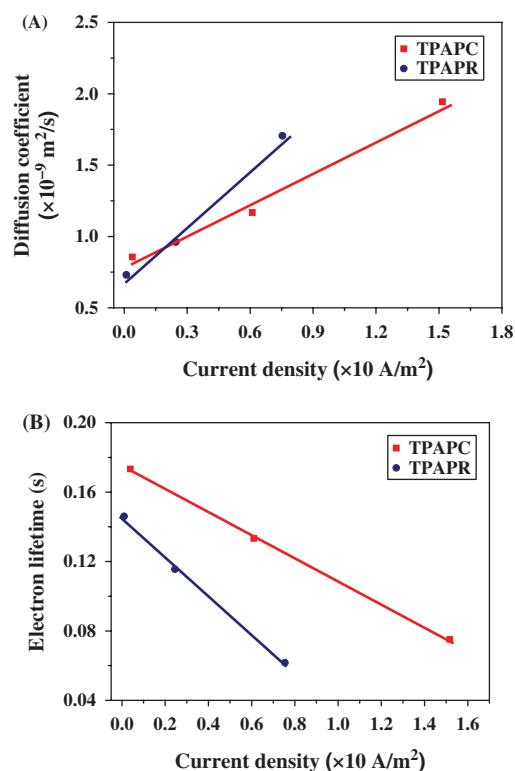


Figure 6. Electron diffusion coefficient versus photo current density (A) and electron lifetime versus the photo current density (B) for DSSCs using TPAPC and TPAPR as sensitizers.

intensity condition, the laser beam was controlled on/off to record the decay in the photocurrent density and voltage as a function of time.^{23,24}

Figure 6(a) presents the relationship between the diffusion coefficient (D_n) and current density of the TPAPC and TPAPR sensitized solar cells. The TPAPC devices show the higher current density and diffusion coefficient under the same light intensity conditions compared to TPAPR device. Figure 6(b) shows that TPAPC has a longer electron lifetime than TPAPR. The higher D_n and the longer electron lifetime (τ_e) of the DSSCs using TPAPC as a sensitizer indicate faster electron transport and less electron recombination, respectively, which result a higher photocurrent density and photo-voltage. In addition, the electron diffusion length, L_n , the overall electron collection efficiency (φ_{coll}), and the electron recombination time were calculated using Eq. (4),^{23,24} which shows that the average diffusion length of the TPAPC device is 12.24 μm higher than that of TPAPR 10.37 μm , and the average diffusion length in both cases is higher than the thickness of the photo electrode, 7.5 μm (Table III).

$$L_n = (D_n \tau_e)^{1/2} \quad (4)$$

These results show good agreement with the much higher photo current density of the DSSCs employing TPAPC than that of TPAPR. To determine the reason for the improved V_{OC} of the TPAPC device compared to the TPAPR device,

the EIS were conducted under dark conditions with a forward bias of -0.7 V in the frequency range, 0.1 Hz to 100 kHz (Fig. 5(b)). The impedance spectra were fitted with the equivalent circuit (Fig. 5(b)) to extract the recombination resistance (R_{rec}) (Table III) between the injected electron in TiO_2 nanoparticle and oxidized species (I_3^-) in the electrolyte and the results show a much larger R_{rec} in the case of DSSCs using TPAPC (64.3 Ω) than DSSCs using TPAPR (14.0 Ω). The larger R_{rec} value indicates the reduced potential lost in the solar cells, which results in a higher V_{OC} value for TPAPC. These results show that cyanoacetic acid has stronger electronic coupling with TiO_2 and a lower recombination rate compared to the rhodanine-3-acetic acid acceptor group, which resulted from the broken conjugation due to the methylene group in the rhodanine-3-acetic acid;¹ thus, the solar cell based on TPAPC shows better photovoltaic performance.

4. CONCLUSION

Phenothiazine-triphenylamine dyes (TPAPC and TPAPR) were designed and synthesized, and the effects of different acceptor groups on the optical, electrochemical, and photovoltaic properties were studied. Under illumination conditions, the DSSCs based on TPAPC showed an overall conversion efficiency of 2.66% compared to 1.12% for the DSSCs based on TPAPR. The conversion efficiency was improved significantly by replacing rhodanine-3-acetic acid with cyanoacetic acid, which can be attributed to the higher J_{SC} and V_{OC} of the TPAPC device. The reason for this is the cyanoacetic acid anchoring group on TiO_2 with the coordinated triphenylamine-phenothiazine sensitizer showed relatively efficient electron injection, as evidenced by the electrochemical impedance and stepped light induced measurement analysis. The results suggest that cyanoacetic acid acceptor results in DSSCs with better properties than the rhodanine-3-acetic acid acceptor in phenothiazine-triphenylamine dyes.

Acknowledgment: This study was supported by the “New and Renewable Energy Core Technology Program” of the Korea Institute of Energy Technology Evaluation and Planning (KETEP) granted financial resource from the Ministry of Trade, Industry and Energy, Republic of Korea (No. 20133010011750). This study was also supported by “Human Resources Program in Energy Technology” of the Korea Institute of Energy Technology Evaluation and Planning (KETEP), granted financial resource from the Ministry of Trade, Industry and Energy, Republic of Korea (No. 20154030200760).

References and Notes

1. A. Hagfeldt, G. Boschloo, L. Sun, L. Kloo, and H. Pettersson, *Chem. Rev.* 110, 6595 (2010).
2. M. I. Abdullah, M. R. S. A. Janjua, A. Mahmood, S. Ali, and M. Ali, *Bull. Korean Chem. Soc.* 34, 2093 (2013).

3. S. Agrawal, M. Pastore, G. Marotta, M. A. Reddy, M. Chandrasekharam, and F. D. Angelis, *ACS Appl. Mater. Interface* 5, 12469 (2013).
4. S. Hwang, J. H. Lee, C. Park, H. Lee, C. Kim, C. Park, M.-H. Lee, W. Lee, J. Park, K. Kim, N.-G. Park, and C. Kim, *Chem. Commun.* 46, 4887 (2007).
5. J. Song and J. Xu, *Bull. Korean Chem. Soc.* 34, 3211 (2013).
6. W. Wu, J. Yang, J. Hua, J. Tang, L. Zhang, Y. Long, and H. Tian, *J. Mater. Chem.* 20, 1772 (2010).
7. S. Nakade, T. Kanzaki, W. Kubo, T. Kitamura, Y. Wada, and S. Yanagida, *J. Phys. Chem. B* 109, 3480 (2005).
8. T. Marinado, D. P. Hagberg, M. Hedlund, T. Edvinsson, E. M. J. Johansson, G. Boschloo, H. Rensmo, T. Brinck, L. Sun, and A. Hagfeldt, *Phys. Chem. Chem. Phys.* 11, 133 (2009).
9. Z. Wan, C. Jia, Y. Duan, J. Zhang, Y. Lin, and Y. Shi, *Dyes and Pigments* 94, 150 (2012).
10. H. Shang, Y. Luo, X. Guo, X. Huang, X. Zhan, K. Jiang, and Q. Meng, *Dyes and Pigments* 87, 249 (2010).
11. Z. Wan, C. Jia, Y. Duan, L. Zhou, Y. Lin, and Y. Shi, *J. Mater. Chem.* 22, 25140 (2012).
12. M. Liang, W. Xu, F. Cai, P. Chen, B. Peng, J. Chen, and Z. Li, *J. Phys. Chem. C* 111, 4465 (2007).
13. Z. Q. Wan, C. Y. Jia, J. Q. Zhang, Y. D. Duan, Y. Lin, and Y. Shi, *Journal of Power Sources* 199, 426 (2012).
14. Z. Wan, C. Jia, Y. Duan, L. Zhou, J. Zhang, Y. Lin, and Y. Shi, *RSC Advances* 2, 4507 (2012).
15. A. Shafiee, M. M. Salleh, and M. Yahaya, *Sains Malaysiana* 40, 173 (2011).
16. Y. S. Yang, H. D. Kim, J.-H. Ryu, K. K. Kim, S. S. Park, K.-S. Ahn, and J. H. Kim, *Synthetic Metals* 161, 850 (2011).
17. X. Chen, C. G. Jia, Z. Wan, J. Zhang, and X. Yao, *Spectrochimica Acta Part A: Molecular and Biomolecular Spectroscopy* 123, 282 (2014).
18. J. H. Park, B. Y. Jang, S. Thogiti, J.-H. Ryu, S.-H. Kim, Y.-A. Son, and J. H. Kim, *S. Met.* 203, 235 (2015).
19. T. Suresh, R. K. Chitumalla, N. T. Hai, J. Jang, T. J. Lee, and J. H. Kim, *RSC Adv.* 6, 26559 (2016).
20. P. Wang, C. Klein, R. Humphry-Baker, S. M. Zakeeruddin, and M. Grätzel, *J. Am. Chem. Soc.* 127, 808 (2005).
21. D. Kuang, C. Klein, S. Ito, J.-E. Moser, R. Humphry-Baker, S. M. Zakeeruddin, and M. Grätzel, *Adv. Funct. Mater.* 17, 154 (2007).
22. J. Li, W. Xu, and Y. Shi, *Transaction On Control And Mechanical Systems* 1, 235 (2012).
23. S. Nakade, T. Kanzaki, Y. Wada, and S. Yanagida, *Langmuir* 21, 10803 (2005).
24. K.-S. Ahn, M.-S. Kang, J.-K. Lee, B.-C. Shin, and J.-W. Lee, *Appl. Phys. Lett.* 89, 013103-1 (2006).

Received: 12 January 2016. Accepted: 12 September 2016.

Delivered by Ingenta to: State University of New York at Binghamton
IP: 188.72.127.123 On: Mon, 06 Mar 2017 08:55:58
Copyright: American Scientific Publishers